Swiss J Geosci (2011) 104 (Suppl 1):S35–S55
DOI 10.1007/s00015-011-0073-1

The oldest azhdarchoid pterosaur from the Late Jurassic Solnhofen Limestone (Early Tithonian) of Southern Germany

Eberhard Frey · Christian A. Meyer · Helmut Tischlinger

Received: 20 October 2009 / Accepted: 25 May 2011 / Published online: 18 October 2011

Abstract Based on an almost complete three-dimensionally preserved skeleton, a new genus and species of an azhdarchoid pterosaur *Aurorazhdarcho primordius* n.gen. n.sp. from the Late Jurassic Solnhofen limestone (Early Tithonian) of the Eichstätt area (Bavaria, Germany) is described. Furthermore, a new family the Protazhdarchidae is proposed. The specimen is attributed to the Azhdarchoidea based on its glenoid fossa level with the sternum, the shovel-like shape of the sternal plate, the wide furca of the coracoid, the metacarpus being longer than radius and ulna, the femur being 1/3 longer than the humerus, the femorotibial ratio, and the hammer-shaped humerus among other diagnostic features. Under UV-light, soft tissue preservation around the external mould of the head is visible. It consists of tiny flakes possibly remnants of skin. The dorsally curved outline of the external mould of the head suggests the presence of a cranial crest. The new species is the oldest record of the azhdarchoid pterosaurs. It supports the Eurasian origin of this group that includes the largest flying animal ever.

Keywords Azhdarchoidea · Pterosauria · Soft tissue preservation · Tithonian · Southern Germany

Zusammenfassung Basierend auf einem fast vollständigen, drei-dimensional erhaltenen Skelett wird die neue Gattung und Art eines azhdarchoiden Pterosauriers *Aurorazhdarcho primordius* n.gen. n.sp. beschrieben. Gleichzeitig wird die Familie Protazhdarchidae vorgeschlagen. Das Stück stammt aus den spätjurassischen Solnhofener Plattenkalken (frühes Tithonium) aus der Umgebung von Eichstätt (Bayern, Deutschland). Das Schultergelenk in Höhe des Sternum, die schaufelförmige Sternalplatte, die weite Coracoidgabel, der Metacarpus, der länger ist als Radius und Ulna, der Femur, der um ein Drittel länger ist als der Humerus, das femorotibiale Längenverhältnis und der hammerförmige Humerus und andere diagnostische Charakteristika erlauben die Zuordnung des Fundes zu den azhdarchoiden Pterosauriern. Unter UV-Licht ist Weichteilerhaltung im Bereich des Kopfabdruckes sichtbar, die aus winzigen Flocken besteht und als mögliche Überreste der Haut interpretiert werden. Der gewölbte Rand im Dorsalbereich des Kopfabdruckes macht einen Scheitelkamm wahrscheinlich. Die vorliegende neue Art ist der älteste Nachweis für die azhdarchoiden Pterosaurier und untermauert den eurasischen Ursprung dieser Flugsauriergruppe, aus der die größten bekannten Flugtiere aller Zeiten hervorgingen.

Editorial handling: Jean-Paul Billon-Bruyat.

E. Frey (✉)
Staatliches Museum für Naturkunde, Erbprinzenstrasse 13, 76113 Karlsruhe, Germany
e-mail: dinofrey@aol.com

C. A. Meyer
Naturhistorisches Museum, Augustinergasse 2, 4001 Basel, Switzerland

H. Tischlinger
Tannenweg 16, 85134 Stammham, Germany

Institutional abbreviations

MNHS	Museum of Natural History Sintra, Portugal
NMB	Naturhistorisches Museum Basel, Switzerland
SMNK	Staatliches Museum für Naturkunde Karlsruhe, Germany

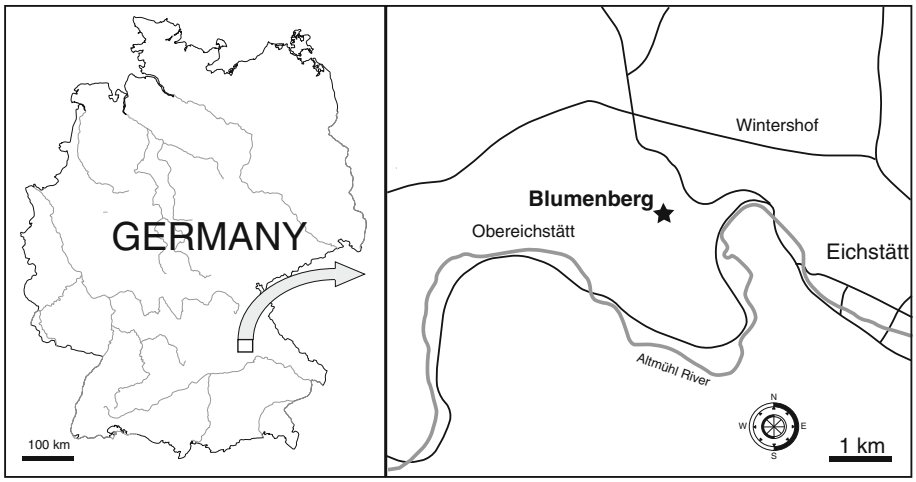

Fig. 1 Geographic location of the Blumenberg Quarry (*asterisk*) near Eichstätt (Bavaria, Germany) where the holotype of *Aurorazhdarcho primordius* was discovered

Introduction

During the Late Cretaceous, azhdarchoid pterosaurs reached enormous wingspans of 10–14 m and thus were the largest flying animals ever. The oldest records of Azhdarchoidea comes from the Early Cretaceous (Aptian) Jiufotang Formation of Liaoling, China (He et al. 2004) with the genera *Sinopterus, Chaoyangopterus, Jidapterus, Shezhaupterus* and *Huaxiapterus* (Li et al. 2003; Wang and Zhou 2003a, b, 2006; Lü and Yuan 2005; Lü and Ji 2006; Lü et al. 2006, 2007, 2008; Unwin 2006), and from the coeval Crato Formation of Northeastern Brazil with the genera "*Tapejara*" and *Tupandactylus* (Kellner 1989; Kellner and Campos 2007; Unwin and Martill 2007). With their first appearance in the fossil record the Azhdrachoidea show a surprising diversity and inhabited both Laurasia and Gondwana. Most likely, the largest of these early Azhdarchoids reached wingspans of no more than 3 m. According to Lü and Ji (2006), *Eoazhdarcho liaoxinensis* (Lü and Ji 2005) from the Jiufotang Formation, China, together with *Eopteranodon* represent "potentially primitive" [*sic*] azhdarchoids, forming the outgroup of the Azhdarchoidea. However, there is no discussion of this topic and the key features that would refer the two species to primordial azhdarchoids are not referenced. Azhdarchoid pterosaurs share enigmatic features, which are unique among their kin: the distal wing finger phalanges show a T-shaped cross-section, the femur is longer than the humerus, the tibia is about two-thirds longer than the femur resulting in a deep wing, the wings articulated level with the mid chest or the sternum, and the neural canal is integrated in the tubular vertebral body, which is confluent with the neural arch.

The low wing articulation combined with a low aspect ratio probably made the azhdarchoid construction exceedingly manoeuvrable, compared to the ornithocheirid construction. Here, we report on a Late Jurassic pterosaur, which shows a remarkable similarities with the azhdarchoid construction.

The specimen was discovered by a private collector (Peter Katschmekat) in 1998 in the public Blumenberg Quarry, 3 km northwest of Eichstätt (11°53′47 50″N, 11°08′54.47″; Fig. 1), and was prepared by Gerd Stübener. The specimen comes from the Solnhofen Lithographic Limestone (Upper Eichstätt Formation, Early Tithonian) in Bavaria (Southern Germany) and represents the oldest known azhdarchoid pterosaur. While the postcranium is completely preserved in three dimensions and mostly articulated, skull and neck are missing (Figs. 2, 3). However, these parts left an external mould on the slab showing the outline of the head and neck in a cloud of organic matter, consisting of tiny flakes when observed under UV-light (Fig. 4a). This type of soft part preservation is hitherto unknown in pterosaurs.

UV light photography

Most skeletal remains of fossils and slightly mineralized soft parts from the Late Jurassic plattenkalks of southern Germany are fluorescent under ultraviolet radiation. Many times details of skeletal remains as well as soft parts can be more precisely investigated in ultraviolet light than in visible light. Delicate skeletal elements including different bony components and remains of soft parts sometimes are poorly or not discernable in visible light but illuminate conspicuously under filtered UV. Each limestone slab and bone or tissue will react differently to different light wave lengths and has to be captured differently with varying exposure times and filters. A correct combination is needed to highlight the area of interest (Tischlinger 2002, 2005).

For the ultraviolet-light investigation of *Aurorazhdarcho primordius* we used a set of UVA lamps with a wavelength of 365–366 nm and an intensity between 4,000 and more than 50,000 microwatts per 10 mm^2, depending on the

Fig. 2 *Aurorazhdarcho primordius* n.gen. n.sp., holotype (NMB Sh 110) from the Solnhofen Plattenkalk, Blumenberg Quarry near Eichstätt (Bavaria, Germany). *Scale bar* 50 mm

distance concerned and the number of lamps. The application of different filters allowed a selective visualisation of peculiar fine structures, here the soft tissue flakes. For this, a set of different color correction filters was necessary. The optimum filtering was tested in a series of experiments. In addition the number and combination of filters were subject to the displacement, intensity, and incident angle of the ultraviolet lamps. Documentation via ultraviolet-light photography was solely executed by means of analogue photography on slide film.

Preservation

The specimen NMB Sh 110 is preserved on a single slab, which measures 550 × 480 mm and has been prepared from the bottom side, after the brittle and marly bottom slab had been re-glued. This is the reason why all bones are preserved in three dimensions. The specimen preserves all postcranial elements. The skull and the vertebral column of the neck are missing but are visible as an external mould. The neck was curved dorsally at a right angle with respect to the trunk and articulated with the head from ventrally. Under UV-light the external mould of head and neck is outlined by organic matter consisting of tiny flakes of calcium phosphate, which are luminescent (Fig. 3). The imprints of the open jaws, the right eye, the neck, throat pouch and probably a head crest are visible in a way that the shape and size of the head can be reconstructed to certain reliability. Corrosion of the skeleton is only visible in few places, especially on both femora and the right wing finger metacarpal.

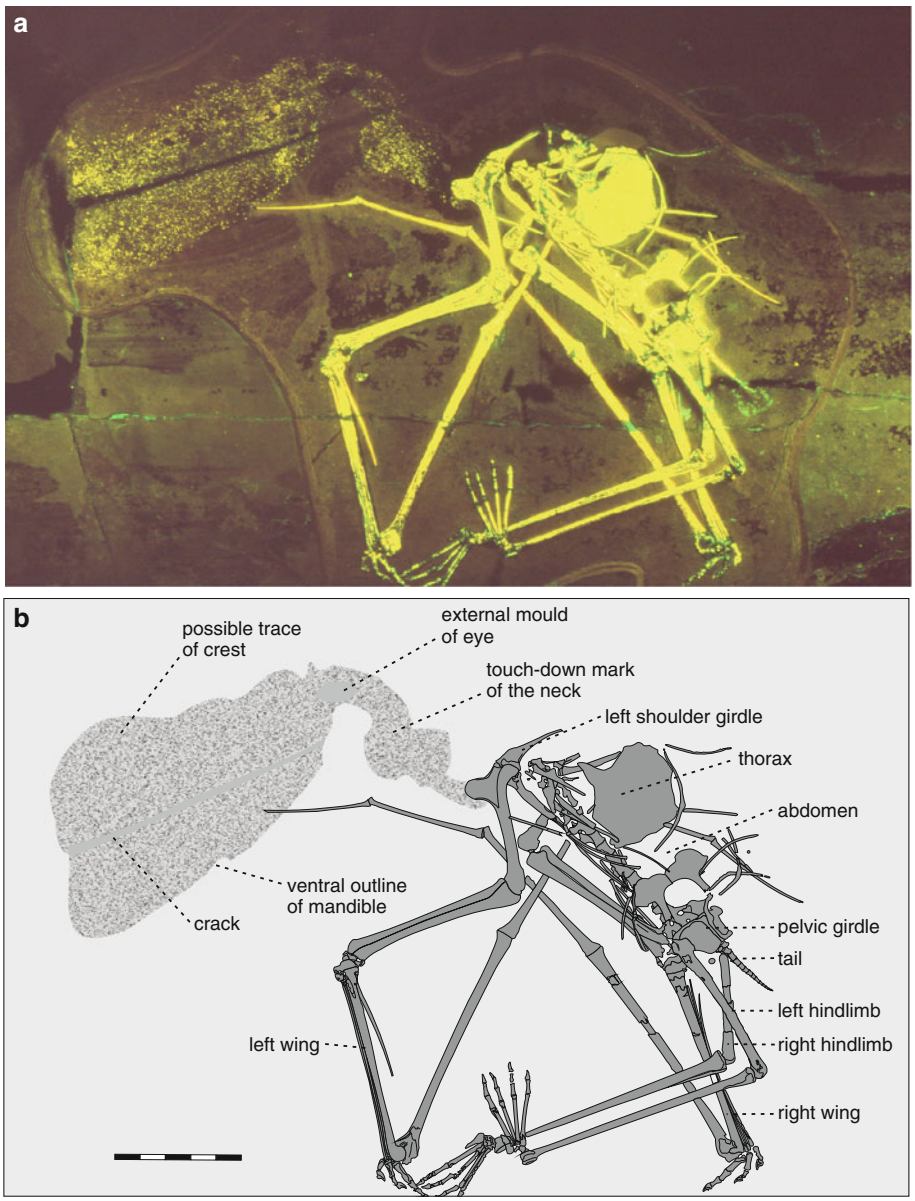

Fig. 3 *Aurorazhdarcho primordius* n.gen. n.sp., holotype (NMB Sh 110). **a** Under UV light with luminescent soft tissue traces; **b** line drawing of the skeleton and the soft tissue preservation as seen under UV-light. *Scale bar* 50 mm

The skeleton of the trunk is seen from lateroventrally with the right side up (Figs. 2, 3). It obscures the left scapulocoracoid, the proximal half of the left humerus, the distal half of the right wing finger phalanx II and the proximal half of the third. The vertebral column of thorax, sacrum and tail are preserved in their anatomical positions.

The bones of the extremities are mostly articulated, too, but some joints are distorted beyond normal articulation. The caudal third of the left side of the rib cage and the gastric basket are completely dismembered. Gastralia and ribs from the left body side lie scattered between the caudal margin of the sternum and in the vicinity of the pelvic girdle. They overlie the distal phalanges of the left wing and the distal portion of the left radius/ulna. The prepubic bones are slightly shifted cranially from their articulation with the pubic bones. Their alae are in contact at the medial margin.

The right lumbar ribs of the vertebral segments XI and X are articulated with their respective vertebrae, but have rotated caudally thereby losing the contact to the sternum. All other lumbar ribs are scattered in the area that once formed the abdominal cavity. The same holds true for the gastralia.

The sternum lies close to its original position and is seen from ventrally. Both coracoids are separated from their articulation with the base of the cristospine. The sternum has slid to the left side of the vertebral column. The bone obscures the ala of the left scapula.

The right scapulocoracoid is articulated and seen from caudally. It has rotated cranially around the apex of the

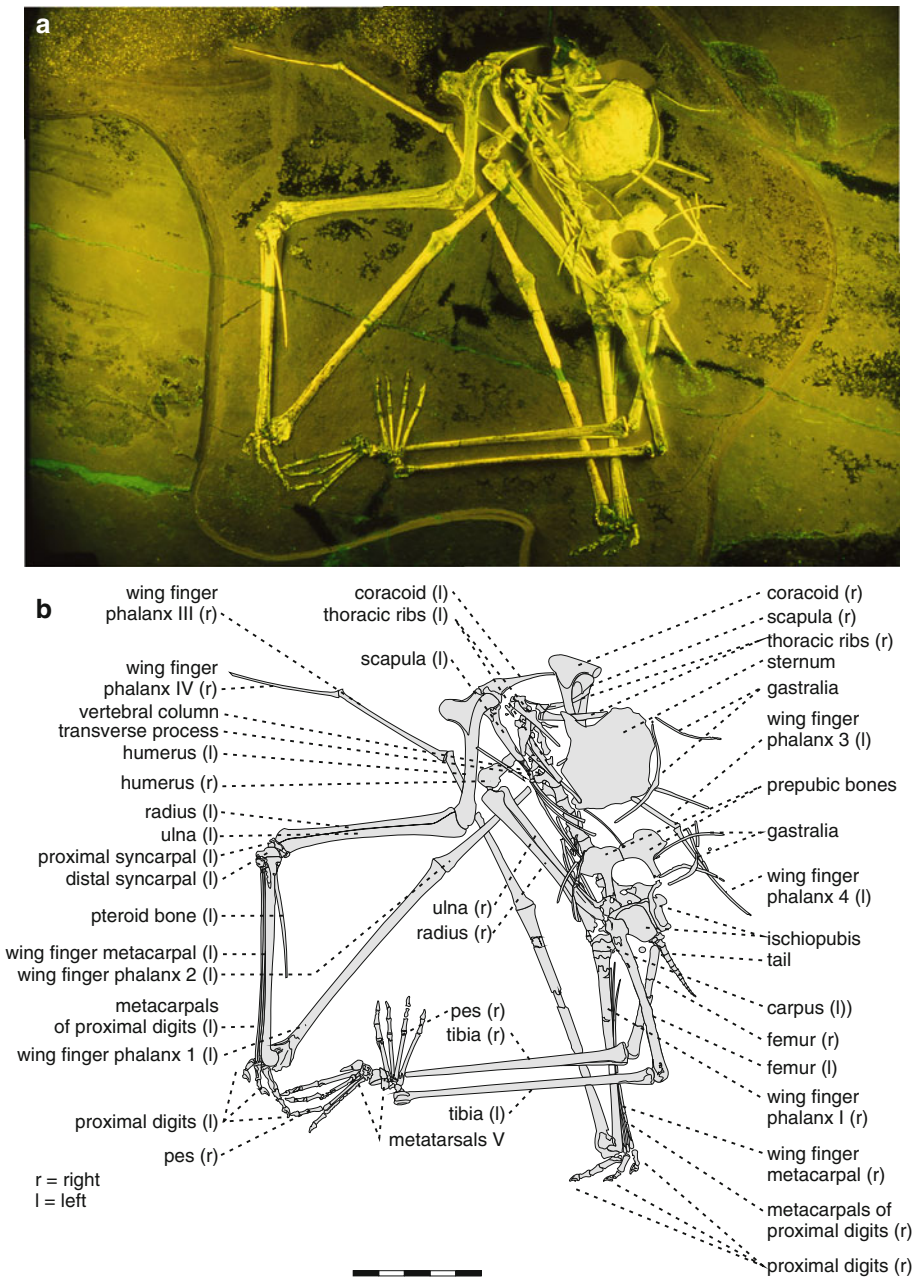

Fig. 4 *Aurorazhdarcho primordius* n.gen. n.sp., holotype (NMB Sh 110), close up of the skeleton. **a** Under UV-light, *greenish lines* and patches are glue; **b** Line drawing of the skeleton. *Scale bar* 50 mm

scapula, which lies close to its in situ position adjacent to the thoracic vertebral column level with thoracic vertebra 5.

The head of the right humerus articulates with the glenoid fossa and shows its ventral aspect, as do all bones of the right wing. The angle between humerus and radius/ulna as well as the angle formed by radius/ulna and the metacarpus is about 100°. The metacarpus and wing finger phalanx I include an angle of about 35°. Wing finger phalanx I and II form a straight line. The distal two wing finger phalanges are bent cranially at an angle of 90° against wing finger phalanx II and are articulated with each other in slight hyperextension. The tip of the right pteroid bone faces distally and forms an angle of about 10° with the metacarpus.

The left coracoid is orientated at an angle of 45° caudally with respect to the surface of the slab and is prepared from all sides. A small patch of matrix covers the medial face of the articular furca with the cristospine. This part of the left coracoid is slightly plastically deformed. The scapular part of the glenoid fossa lies in full articulation, but the entire corpus and the ala of the left scapula are obscured by matrix, the two cranial-most ribs from the left side of the thorax and the sternum.

The left wing is seen from the ventral side. The elbow joint is angled at 90°, while the carpal joint includes about

150°. Wing finger phalanx I is flexed against the metacarpus at an angle of 20° and lines up straight with wing finger phalanx II. The distally following joints are slightly hyperextended at an angle of 150°.

The three small digits of both wings show their palmar aspect. They are all bent distally. The phalanges are lined up straight. Only the phalanges of the second digit of the left manus show a slight hyperextension, so do the ungual phalanges of the small digits in both manus. All small digits include an angle of about 20°–30°. While the metacarpals of the small digits of the right manus are fully articulated, those of the left are separated from their carpal articulations, but otherwise in place.

The right femur is seen from laterally and stands at right angle to the tibia. The tibia has rotated 90° around its long axis laterally so that it is seen from craniomedially. The tarsus has disarticulated from the distal tibial roller joint, but the connection with the metatarsus is still close to its original position. The pes with the articulated tarsals lies medially adjacent to the distal tibial roller joint on its dorsal face in a 90° supination. Its middle long axis is orientated at 90° against the tibia. The metatarsals I through III are spread at angle of about 10°. The angle between metatarsals III and IV is about 7°. The pedal phalanges are in line with the metacarpals respectively with the exception of the ungual phalanges of digits I and II which are slightly displaced laterally. Metatarsal V lies adjacent to metatarsal IV.

The left femur has rotated dorsomedially and lies now underneath the dorsal face of the sacrum facing caudomedially. It is seen from its medial face. The left tibia forms an angle of about 100° with the femur and exposes its craniolateral surface, so that the fibula is visible adjacent to the lateral face of the proximal fifth of the tibia. The distal tibial roller joint is fully exposed in cranial view. The tarsus is disarticulated from the distal tibial roller but remained in articulation with the metatarsals. The left pes as a whole is angled at about 160° against the tibia and lies on its dorsal face. While metatarsals I and II lie adjacent to each other, the metatarsals II-IV include angles of about 8°. The 5th metatarsal is spread laterally by 2°. The phalanges of the pedal digits I and IV lie in line with their metatarsals, whereby those of digit I are slightly separated. The phalanges of the digits II and III are angled laterally at about 170° and lie parallel to each other.

Systematic palaeontology

Pterosauria Kaup 1834

Azhdarchoidea Unwin 1995

Protazhdarchidae nov. fam.

Aurorazhdarcho n.gen.

Aurorazhdarcho primordius n.sp.

Derivatio nominis: Genus name from Latin *aurora* = dawn and Kirgisian *azhdarcho* = dragon; species name from Latin *primordius* = the earliest

Holotypus: A single articulated skull- and neckless specimen housed in the Natural History Museum Basel (Switzerland) under the collection number NMB Sh 110 (Figs. 2, 3)

Locus typicus: Blumenberg Quarry near Eichstätt (Bavaria, Germany; Fig. 1)

Stratum typicum: Solnhofen Lithographic Limestone (Upper Eichstätt Formation, Late Jurassic, Lower Tithonian, Hybonotum Zone; Schweigert 2007).

The specimen is referred to the Azhdarchoidea according to the following combination of features (Lawson 1975; Nessov 1984, 1991; Unwin 1995, 2003; Martill et al. 1998; Kellner 2003):

1. Glenoid fossa lies ventral to the vertebral column (Fig. 5; Frey et al. 2003a);
2. Femur longer than humerus (ratio humerus/femur = 0.79; Table 1; Fig. 6);
3. Tibia more than 1/3 longer than femur (ratio femur/tibia = 0.98; Table 1; Fig. 6);
4. Deltopectoral crest situated in the proximal fourth of the humerus and protruding at right angles from the shaft of the humerus; proximal and medial margins of the deltopectoral crest parallel to each other, cranial margin convex;
5. Sternal plate shovel-shaped with three lateral pits for sternal rib segments (Figs. 2, 3);
6. Cristospine less than 1/5 the length of the sternal plate (Figs. 2, 3);
7. Furca of the coracoid almost twice as wide as the narrowest part of the shaft, which is visible on the right coracoid (Figs. 2, 3);
8. Second wing finger phalanx with a groove on its palmar face. This groove might be indicative for a crest on the dorsal side, but this is hidden by matrix.

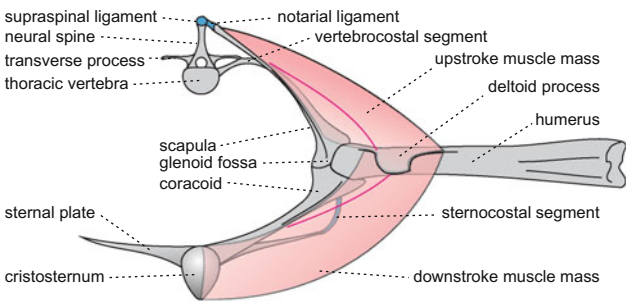

Fig. 5 *Aurorazhdarcho primordius* n.gen. n.sp.: schematic reconstruction of the shoulder girdle in cross-section. Note the low wing attachment, which is indicative for an azhdarchoid pterosaur construction

Table 1 *Aurorazhdarcho primordius*: table of measurements of the forelimbs and hind limbs (in mm)

Forelimb	Right	Left	Hind limb	Right	Left
Humerus	62.4	?	Femur	79.0	74.0
Radius	80.8	80.2	Tibia	116.0	115.0
Ulna	82.9	?	Fibula	?	40.0
Carpus	7.0	?	Tarsus	4.0	4.2
1st metacarpal	86.5	?	Metatarsal I	22.6	24.0
2nd metacarpal	87.0	?	Metatarsal II	22.6	23.0
3rd metacarpal	?	?	Metatarsal III	20.5	21.6
4th metacarpal	94.6	94.0	Metatarsal IV	19.5	19.5
Pteroid bone	54.2	?	Metatarsal V	7.3	10.8
Digit 1 phalanx 1	6.0	6.4	Digit 1 phalanx 1	6.2	6.7
Digit 1 ungual	4.4	4.0	Digit 1 ungual	4.3	5.0
Digit 2 phalanx 1	6.4	7.1	Digit 2 phalanx 1	5.0	6.5
Digit 2 phalanx 2	4.5	4.5	Digit 2 phalanx 2	4.4	5.0
Digit 2 ungual	4.0	4.5	Digit 2 ungual	4.3	4.8
Digit 3 phalanx 1	10.1	10.3	Digit 3 phalanx 1	6.5	7.0
Digit 3 phalanx 2	5.4	5.5	Digit 3 phalanx 2	3.8	5.8
Digit 3 phalanx 3	5.3	4.8	Digit 3 ungual	3.2	4.5
Digit 3 ungual	4.1	3.3			
Digit 4 phalanx 1	120.0	119.0	Digit 4 phalanx 1	6.7	7.1
Digit 4 phalanx 2	?	70.8	Digit 4 phalanx 2	6.0	6.5
Digit 4 phalanx 3	?	50.6	Digit 4 ungual	3.6	0.8
Digit 4 phalanx 4	50.3	50.5			

?, no measurement possible

Diagnosis of family and genus

Pterosaur of azhdarchoid flight configuration, but differs from all members of the Azhdarchidae in the following features:

1. Wing finger metacarpal as long as the radius as ulna (Table 1; Fig. 6; longer in the Azhdarchidae);
2. Wing finger phalanges III and IV together longer than wing finger phalanx II (Table 1; Fig. 6; shorter in the Azhdarchidae);
3. Palmar aspect of the two distal wing finger phalanges convex (concave in the Azhdarchidae);
4. Lateral crests dorsal and ventral to the glenoid fossa missing (Fig. 5; prominent in the Azhdarchidae);
5. No pneumatic foramen perforating the ventral face of the humeral neck;
6. All thoracic ribs articulated with their vertebrae (at least three cranial-most thoracic ribs fused to their vertebrae in adult Azhdarchidae).

Because these features are different from the known configuration in Azhdarchidae, we propose to erect a new family, the Protazhdarchidae, because most of the diagnostic features of *Aurorazhdarcho* reflect an early state of evolution within the azhdarchoid construction. The reasons for this approach are discussed below.

Diagnosis of species

As for the family and genus.

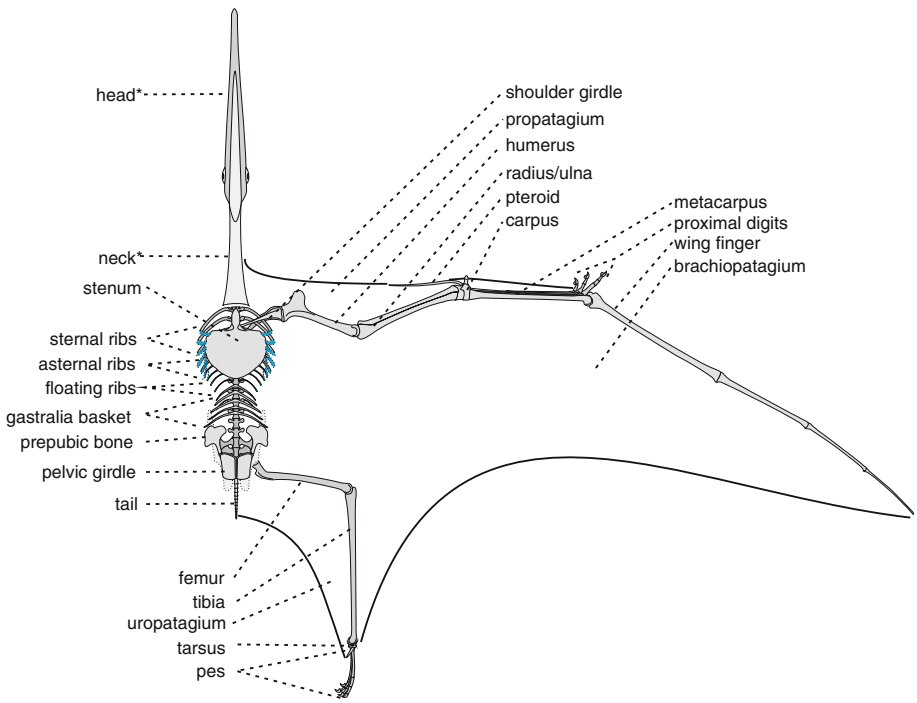

Fig. 6 *Aurorazhdarcho primordius* n.gen. n.sp.: reconstruction of *Aurorazhdarcho primordius* n.gen. n.sp in ventral aspect. The *asterisks* indicate the body parts that are reconstructed from the soft tissue patch and the external moulds

Description

Vertebral column (Figs. 2, 3)

Thoracolumbar vertebrae

The presacral vertebral column as preserved consists of 14 vertebrae. Eleven of them are bearing ribs. Therefore, the lumbar region comprises three vertebrae, which are overlain by the left prepubic bone. All vertebral centra are seen in ventral aspect. They are of almost equal size and show a strong constriction giving a hourglass-shaped outline. The minimum diameter in the middle of the circumvertebral constriction is about two-thirds of the maximum diameter at the articular face. The intervertebral articulations fit so closely that there was no space for an intervertebral annulus fibrosus. The centrum of the first vertebra shows a median ventral sulcus, which extends caudally for 1/5 the length of the centrum. The sulcus divides the ventral face of the articular face into two halves. The cranial-most part of the vertebral sequence is dislocated in cranial direction and turned dorsally, so that the ventral third of the caudal articular condyle is visible. The bases of the transverse processes and adjacent prezygapophyses are only exposed on the left side of the sixth and seventh, as well as the ninth and tenth vertebra. The ventral surface shows a transverse depression that medially continues into a shallow pleurocoel, which is also visible in vertebra six and nine. Cranially and caudally the depression is bordered by sharp ridges, which taper at the lateral margin of the transverse process.

Sacral vertebrae

Only the two cranial-most vertebrae and the caudal end of the last sacral vertebrae are visible. The centrum outline of the sacral vertebra I is hourglass-shaped in ventral view. Its cranial face is 1/3 wider than the caudal one and twice as wide as the narrowest diameter of the constriction. The sacral ribs emerge from the craniolateral half of the vertebra and extend caudolaterally at an angle of 60°. They are co-ossified with the centrum and the ilium. While the cranial margin is regularly concave, the caudal margin of the first sacral rib shows two concavities. The medial one is 1/4 the size of the lateral one and forms the cranial border of the first sacral foramen and the lateral one forms the contact facet for the second right sacral rib. The base of the first sacral rib on the right is hidden by the peduncle of the right prepubis. Its distal terminus is not visible.

The centrum of the second sacral vertebra is less constricted than the first one and is dorsoventrally flattened. It is co-ossified with the first sacral vertebra in a way that only a faint trace of an intervertebral joint is visible (Fig. 6). The second pair of sacral ribs is co-ossified with the cranial half of the lateral face of the vertebral corpus and, with the craniomedial corner contacts the caudolateral corners of the corpus of the first sacral vertebra. The caudal terminus of the lateral margin of the right second sacral rib is obscured by the ischiopubic bones. Both the cranial and caudal margins of the second sacral rib are concave. The caudal margin forms the cranial border of the second sacral foramen. The concave cranial margin of this sacral rib borders the second sacral foramen caudally. Of the caudal-most sacral vertebra only the circular slightly convex articular condyle for the first caudal vertebra is visible.

Caudal vertebrae

The vertebral column of the tail consists of fourteen vertebrae. All of them are seen in ventral aspect. The first caudal vertebra is 1/5 longer than wide. Its minimal diameter at its constriction is less than 1/5 of the diameter at the cranial articular face. The caudally following vertebrae until number seven are almost cylindrical and about 1/3 longer than wide. The minimal diameter is 1/4 of the maximum diameter, which is at the cranial articular face. The terminal articular face is 1/5 to 1/6 less wide than that of the cranial one. The terminal seven caudal vertebrae are conical with the cranial articular face being equal to the vertebral length. Caudal vertebrae five to eight show a deep median sulcus.

Thoracic and abdominal skeleton Ribs (Coastae; Figs. 2, 3, 5)

The ribs of the right body side are well preserved despite their distortion and disarticulation. Only the vertebrocostal elements are preserved. Eleven pairs of ribs formed the thorax. The cranial three are four to five times as thick as the subsequent ones. The capitulum of the three cranial ribs is curving medially at an angle of about 150°. The neck of the rib is about 1/5 to 1/6 the length of the costal corpus. The corpora of the ribs are laterally compressed. Their diameter in transverse direction is about 1/4 of the longitudinal diameter. The shape of the distal terminus of the costal corpora cannot be reconstructed. The size of the three cranial pairs of ribs gradually increases towards caudally. The three pairs of the receptacular facets on the lateral margins of the sternal plate indicate that these three cranial pairs of ribs articulated with the sternum by means of their sternocostal segments. Therefore, these ribs are sternal ribs. The fourth is the longest thoracic rib, but has only 1/4 the diameter of the third rib. The fifth thoracic rib

has the same diameter as the fourth. The costal corpus is stronger curved than that of the previous one. From the seventh thoracic rib caudally the length of the ribs rapidly declines towards the eleventh, which has a little less than half the length of the fourth. The distal terminus of the ribs is missing or covered with matrix.

Gastralia (Figs. 2, 3, 5)

Three gastralia are preserved in such a way that they are identified without any doubt, two more might have been present. They lie scattered in the abdominal region. Therefore, the gastralia basket cannot be reliably reconstructed. The largest gastrale lies along the caudal margin of the sternum with its caudal margin facing cranially. The bone is widely bowl-shaped with the apex facing caudally, being the thickest part of the gastrale. The cranial margin of the gastrale is marked by a triangular median process. Here, the diameter of the bone is 1.5 times the diameter of the corpus. The other two gastralia show a similar shape but are about half the size. The cranial median process is only seen in the second largest gastrale, which lies adjacent to the left side of the pelvis. One of the remaining two possible gastralia lies adjacent to the latter ones, the other on the left side of the sternum.

Sternum (Figs. 2, 3, 4, 5)

The sternum is exposed in ventral aspect. Only a small seam of its right margin is obscured by matrix overlying ribs and parts of the vertebral column. The sternal plate is shovel-shaped in outline with the tip pointing caudally. The caudal margin is irregularly wavy. The right lateral margin is sinusoid with three concavities, which represent the articulation facets with the sternocostal segments of the cranial three thoracic ribs. These articulation facets are separated by two convexities. The cranial margin of the sternal plate runs mediocranially at an angle of 5° on the right and 7° in the left side. Toward medially, the cranial margin merges with the caudodorsal part of the cristospine, whereas the medial concavity on the right is more marked than on the left. The ventral face of the sternal plate is convex with the strongest curvature in the craniomedial portion, where the sternal plate merges with the base of the cristospine. With the exception of three radially arranged compaction grooves on the left half of the sternal plate, and a transverse oval compaction pit adjacent to the left base of the cristospine the ventral face of the sternal plate is smooth. The lateral half of the cranial margin and the interarticular convexities on the lateral margin are both reinforced by a narrow frill. An impression is seen right to the base of the cristospine. The ventral part of the cristospine has broken off, so that the depth of the ventral keel cannot be reconstructed with reliability. The corpus of the cristospine is 1/5 of the median length of the sternal plate. Its lateral faces converge cranially at an angle of about 20°. A pair of blunt caudolaterally directed processes emerges on the lateral face at the base of the cristospine, leaving a constriction at the transition between the sternal plate and the cristospine. These facets are the articulation places for the furca of the coracoids.

Prepubic bones (Figs. 2, 3, 5)

The prepubic bones are seen in ventral aspect. They consist of a caudally facing peduncle, which cranially expands into an ala being approximately six times as wide as the peduncle. The lateral and medial margins of the peduncle are sub-parallel and straight. The caudal margin is marked by a short longitudinal incision in the medial fourth. The lateral two-thirds are smooth. The articular facet is transverse oval, four times wider than high, and slightly concave. It is only exposed on the left prepubic bone.

The medial part of the ala, which is better preserved in the right prepubic bone, has a cranial margin, which is slightly convex in its lateral two-thirds. Towards medially, this convexity gradually increases and meets the caudal margin at an angle of about 90°. The caudal margin is confluent with the medial margin of the peduncle, forming an even concavity. On the right prepubis a blunt, caudally directed tubercle is visible. The lateral part of the ala bulges cranially four times as much as the lateral part. The angle of the cranial incision, which lies in line with the medial margin of the peduncle, is about 90°. The strongly convex craniolateral margin of the lateral part of the ala terminates at the base of a laterally directed rounded process, the caudal part of which is hidden by matrix on the right prepubis. The lateral 2/3 of the caudal margin of the lateral part of the ala is also covered by matrix. On the left prepubis, the lateral part of the ala is deformed and partly missing, so that the caudolateral portion of the prepubis cannot be reconstructed.

Scapulocoracoid (Figs. 2, 3, 4, 5)

The right scapulocoracoidal complex is seen from caudally with most of its lateral face exposed. Scapula and coracoid include an angle of about 70°. Both bones appear to be at least partially fused, because they are not detached from each other despite the cranial rotation of the complex around the tip of the scapula, which still lies close to its anatomical position. The dorsomedial terminus of the scapula is obscured by the capitulum of the fifth thoracic rib and likely ends adjacent to the neural spine of the fifth thoracic vertebra of the sequence. The cranial and caudal

margins of the dorsal two-thirds of the scapular ala slightly diverge toward the glenoid fossa. Then, the cranial margin becomes shallowly concave. Its transition into the glenoidal head of the scapula is overlain by the humerus. The ventrolateral third of the left scapula is marked by a constriction between the scapular ala and the glenoidal head. This constriction is reinforced by a sharp ridge that extends from the deepest point of the caudal convavity and merges with the lateral extremity of the scapular part of the glenoidal surface of the scapular head. Cranially and caudally to this ridge, the bone surface is concave. Of the glenoidal surface only the caudolateral lip is visible, because the humerus lies in articulation with the glenoid fossa. Medially, the glenoidal lip of the scapula is separated from the coracoideal part of the glenoid fossa by a narrow gap.

The ala of the coracoid is directed medially and terminates with a wide and shallow furca, which stands at a right angle to the long axis of the ala. With this furca, the coracoid articulated with the base of the cristospine. The caudal margin of the coracoid is evenly concave and merges with the caudolateral lip of the articular facet of the coracoid. The cranial margin of the coracoidal ala is concave, too, but turns slightly cranially in its lateral third and forms a convex crest, which continues onto a laterally directed tongue-shaped glenoidal process. At the base of this process, a longitudinal depression is visible on the ventral face of the coracoid, which is separated by a blunt ridge in its caudal third. The latter runs obliquely from the caudal margin of the coracoid craniolaterally and merges with the lateral articular process. The lateral glenoidal process interdigitates with the intertubercular sulcus of the humerus. The coracoid is 1/4 shorter than the scapula and less curved.

The left scapulocoracoid is almost vertically embedded. The scapula points in dorsomedial direction. Only its glenoidal portion is visible, which suffered from slight plastic compaction. Of the coracoid, the glenodial portion is preserved with the adjacent base of the shaft, which is oval in cross-section and now faces caudally. The craniomedial half of the coracoidal part of the glenoid fossa is exposed, now facing craniomedially, merging with the tongue-shaped glenoidal process. Medially, a blunt styliform process branches off at an angle of approximately 60°, and lies in articulation with the glenoidal portion of the scapula. This process is twice as large as the tongue-shaped process and separated from the latter by a wide recess forming an angle of about 100°. Again, the coherence of scapula and coracoid suggests at least a partial fusion of the two bones.

Front limb (Figs. 2, 3, 5, 6)

Humerus

The right humerus lies on its dorsal face with the deltopectoral crest facing craniolaterally with respect to the vertebral column. The head of the left humerus is articulated with the glenoid fossa so that the articular surface is not observable. The surface of the ventral epicondyle is damaged. Of the left humerus, only the proximal terminus of the articular head and the distal third of the shaft exposing the distal roller joint or trochlea are seen in cranial aspect. Due to the damaged surface no anatomical details can be observed. The neck of the humerus is angled at about 130° against the shaft in caudal direction. The cranial face of the neck bears a deep intertubercular sulcus, which separates the dorsal tubercular ridge from the ventral one. The ventral tubercular ridge is larger and more vaulted than the dorsal part. The proximal tuberosity of the ventral tubercular ridge is confluent with the articular surface of the head. The margin of the dorsal tubercular ridge runs straight distally along the neck of the humerus, which is 1/8 of the entire humeral length. The deltopectoral crest emerges from the dorsal tubercular ridge at the transition from neck to shaft in cranial direction. The proximal and distal margins of the deltopectoral crest slightly converge; its cranial margin is evenly rounded and its long axis stands at a right angle with the shaft. The longitudinal extension of the deltopectoral crest equals approximately its transverse extension, which is about 1/5 of the humeral length. Its ventral face is smooth. The intertubercular sulcus terminates level with the distal end of the deltoid crest in a pneumatic foramen. Distal to that point the shaft of the humerus is rounded in cross-section and slightly cranially curved. In its distal fifth it bulges toward the epicondyles, where the diameter becomes 1/3 wider than in the shaft. The ventral condyle has the strongest convexity at its distal end.

Ulna

The right ulna is preserved in an anatomical articulation with humerus, carpus and radius of the right wing. Therefore only its ventral aspect is exposed. The left ulna is seen from cranioventrally and its proximal articular face is visible. The distal fourth of the left ulna is obscured by ribs and gastralia. The proximal articular surface shows a trochlear notch, which is separated by a ridge into a ventral and a lateral cotyle. The ventral cotyle is about twice as broad as the lateral one. The anconeal process is as wide as the entire joint and orientated proximally. Its proximal margin is slightly convex in cranial aspect. In ventral view, the anconeal process is triangular with its caudal margin including an angle of about 120° with the caudal margin of the ulna. The cranial margin of the proximal articular face is bordered by a transverse coronoid ridge. A shallow sulcus devides the ventral coronoid tubercle from the dorsal, which has twice the size. From there the ulnar head converges into the shaft with a curvature angle of about

170°. The smallest diameter of the shaft is in the middle, where it comprises half the diameter of the head. Toward distally, the shaft slightly curves caudally. At the articulation with the carpus, the ulna diverges again and, at is distal extremity, is 1/4 wider than in the middle of the shaft. The ventral margin of the distal articular facet is slightly concave. The distoventral styloid process overlaps the cranial corner of the radius.

Radius

Preservation and orientation of the radii equals that of the ulnae. However, the ventral surface of the radii is mostly obscured by the ulnae, as is the ventral part of the proximal articular surface. The head of the radius articulates with the dorsal face of the dorsal glenoidal tuberosity, and contacts the dorsal condyle of the humerus with a semi-lunar articular face, which forms a ridge building the dorsal part of the radial head. From there, the shaft diameter of the radius decreases to about two-thirds of its diameter at the head. The minimal diameter of the radius is in its distal third. Further distally it diverges again toward the distal articular head, of which only the distal margin of the ventral condyle and the ventral styloid process are visible. The blunt ventral styloid process emerges from the caudodistal margin of the articular condyle and wraps the craniodistal extremity of the ulna.

Carpus

The proximal and distal syncarpals are preserved in articulation in both wings and are seen in ventral view. The preaxial carpal is only preserved in the right wing (Fig. 7). It has disarticulated and now lies with is cranial terminus facing distally. Its ventral face is exposed. The proximal margin of proximal syncarpal is irregularly sinusoid. The ventral face of its corpus shows a wavy longitudinal groove and a pit at the cranial third of the distal margin. The distal margin of the articular facet is deeply concave with a blunt, distally orientated process. This concavity accommodates the ventroproximal articulation facet of the distal syncarpal. Toward ventrally, this facet continues onto the caudal part of the corpus of the distal syncarpal. The shape of this part of the corpus is irregularly longitudinally oval and, its surface bears an irregular groove, which runs parallel with the distal margin. The cranial part of the distal syncarpal is transversely oval, 1/3 the size of the caudal part and has an irregular pit in its surface. These two convex parts of corpus are separated by a shallow cotyle, which runs dorsoventrally. This cotyle is the articulation facet for the pteroid. The preaxial carpal is subtriangular in ventral view with bulging lateral margins. The proximal articular facet is three times wider than long. Its medial and lateral

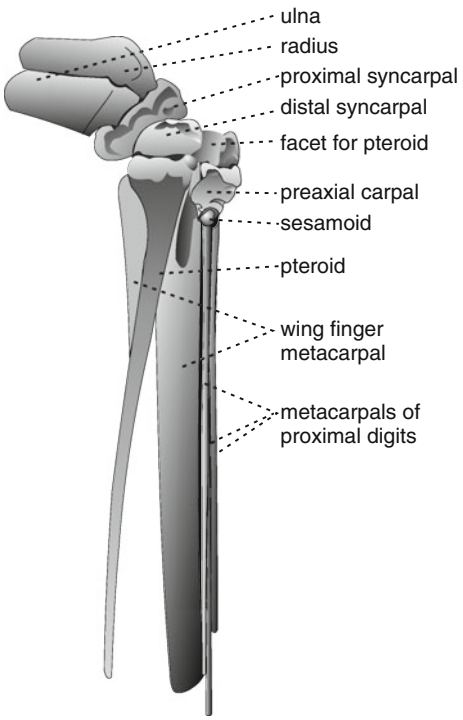

Fig. 7 *Aurorazhdarcho primordius* n.gen. n.sp.: detail of the carpal area of the left wing

margins are concave, as is its dorsal margin with a slight medial convexity on the lateral half. The medial half of the ventral margin is deeply concave, while the lateral half runs straight in ventromedial direction. From the articular surface, the preaxial carpal converges to its apex, which is half as wide as the base of the bone. It bears a subcircular pit, which opens cranioventrally and is occupied by a subglobular sesamoid (Fig. 7).

Pteroid

The right pteroid bone is seen in its caudal aspect (Fig. 7), the left being obscured by bones of the pelvic region. It is disarticulated and faces distally with its tip. The corpus of the pteroid is widest at the articular head, which is 1/9 of the entire length of the corpus. The straight articular surface is seen from craniomedially. It consists of two slightly vaulted condyles of equal size, which are separated by a shallow cotyle and a ventral semiglobular articular head. Dorsal to the middle condyle, there is a cotyle, which is four times as wide as the more ventral one and about twice as deep. The dorsal-most corner of the cotyle continues the ventral semiglobular articular head, which is craniomedially orientated. It is half the size as the middle and ventral condyle and sits in a protuberance, which forms the ventralmost part of the articular surface. From the articular head, the pteroid curves craniomedially, forming a wide,

caudally concave neck, which slightly curves ventrally. It then tapers into the pointed shaft of sub-circular cross-section that slightly curves cranially. The dorsal margin of the shaft is stronger concave than the ventral one.

Metacarpus

Both wing finger metacarpi are exposed in ventral view, but the proximal articulation is only seen in the left one. In the right, this part of the bone is overlain by the preaxial carpal and the pteroid. The metacarpals of the three proximal fingers lie in an anatomical position in the right wing, but are bent in a way that both ends of all three are splayed away from their articulations in cranial direction in the left wing.

Wing finger metacarpal

The external articulation suture with the distal syncarpal is straight and with a narrow interarticular gap. From the articular head towards distally, the bone converges gradually until its distal third, where it shows a minimum diameter, which is about half the diameter at the proximal articulation. Immediately distal to that proximal joint, there is an exalted circumference around at least the ventral half of the bone. The circumference comprises about 1/6 of the length of the bone and is perforated cranioventrally by a long oval pneumatic foramen extending along the long axis of the shaft. The long axis of the foramen is five times the length of its short axis. The caudal face of the wing finger metacarpal appears to be concave in its proximal half. A ridge arising from the caudal edge of the articular head and protruding caudally from under the pteroid suggests this, but in both wing finger metacarpals most of the caudal face is still in the matrix. In the proximal half, the shaft of the wing finger metacarpal is high oval at a ratio of about 1–1.5. Further distally, it becomes rounded, before it slightly diverges by 1/4 to the distal terminus with the articular condyle. Only the ventral face of this condyle is visible, which is superficially damaged. The condyle has twice the width as the shaft at its narrowest point and protrudes caudally. The sulcus between the two condyles begins already on the distal-most dorsal face of the shaft and accommodates the distal termini of the three metacarpals of the small digits. The curvature of the distal condyle of the wing finger metacarpal increases from distally towards caudoproximally.

Metacarpals of the small digits

The metacarpals of the first and the third digit extend from the carpus until the distal end of the shaft of the wing finger metacarpal. The metacarpal of the second small digit appears level with the proximal half of the metacarpus. From what can be seen on the right wing, this metacarpal might not reach the carpus, but tapers somewhere in the proximal third of the metacarpus. The maximum diameter of these three metacarpals is about 1/6 of the smallest diameter of the wing finger metacarpal. The proximal ends of these rod-like, cylindrical bones are rounded so are their distal ends, where they slightly diverge by the factor 1.2. The most cranial situated metacarpal is shortest, the most caudal one has the length of the wing finger metacarpal.

Small digits

In both manus, all phalanges of the small digits are preserved and mostly articulated. The non-ungual phalanges are seen in palmar aspect. Only the basal phalanx of the right digit I is seen in lateropalmar view. All ungual phalanges are exposing their medial face. The phalanges of the three small digits show some surface damage, especially at the articular heads. The planes of the articular surfaces are at right angle to the long axis of their shafts. The basal phalanx of the medial-most digit articulates with the most cranially situated metacarpal. The proximal joint of the basal phalanx is about twice as wide as that of the distal metacarpal condyle. Only the two ventral lips of the articulation facet are preserved, separated by a shallow but sharp incision. They are semi-globular in outline and the medial is 1/3 smaller than the lateral one. The shaft shows a small lateromedially extending bulge adjacent to the proximal articular head. Distal to that bulge, the shaft of the phalanx converges toward the distal roller. The palmar face of the phalangeal shaft is concave as are the medial and lateral margins. In the middle, the shaft reaches its minimal diameter, which is 1/3 of its maximum at the proximal articulation. Towards the distal roller, the shaft slightly diverges again. The distal roller joint of the basal phalanx of the proximal digit is regularly rounded in medial view and expands two times more in palmar direction than in dorsal. The basal phalanx of the second digit is 1/3 longer than that of the first digit. The morphology of the proximal articulation coincides with of the medial-most digit, and the shaft has its minimum diameter in the middle. However, further distally, the shaft expands again to its proximal diameter. The distal double roller is seen in palmar view. The palmar part of the condyles extends proximally over 1/5. The two condyles are of equal size. The morphology of the basal phalanx of the third digit is identical to that of the second, but it is two-thirds longer and 1/4 wider.

The second phalanx of the second digit resembles the basal phalanx of the first digit but is 1/3 shorter. Ventrally on the proximal interphalangeal articulation, the palmar outline of the symmetrical cotylar notches are seen as faint sutures, matching precisely the distal condyles of the basal

phalanx. The distal articulation with the ungual phalanx is identical to that of the basal digit of the proximal-most digit. The palmar aspect of the proximal interphalangeal articulation of the second phalanx of the third digit resembles that of the equivalent phalanx of the second digit, but it is 1/3 wider and the phalanx is 1/3 longer. Its distal double roller is 1/4 the width of the proximal articular trochlea. The shape of the third phalanx of digit three is identical to that of the second phalanx of the second digit but it is 1/4 longer and wider at its proximal articulation.

All three ungual phalanges share the same size and shape. Their length is 2/3 that of the basal phalanx of the proximal-most digit. The medial suture of the proximal cotyle is regularly concave. Dorsal to this cotylar suture, there is a minute proximally pointing extensor tubercle. The dorsal margin of the ungual phalanges is regularly convex until the apex, which lies level with the middle of the cotylar suture in dorsoventral expansion. Palmar to the cotylar suture, there is a semicircular adductor tubercle, which covers about one half of the palmar margin of the ungual phalanx and increases its height by about 1/3 with respect to the cotylar suture. Between the adductor tubercle and the apex, the palmar margin of the ungual phalanx is regularly concave. On the medial face of the ungual phalanx there is a furrow that begins in the centre of the adductor tubercle, then runs parallel to the palmar margin and fades into the ungual apex.

Wing finger

The basal phalanx of the wing finger is 1/5 longer than its metacarpal and preserved in both wings. The proximal articulation is the trochlea of which only the subcircular margin is visible. The caudal articular process is proximally rounded, as is the cranial one, which has twice the size of the caudal. The olecranon process is co-ossified with the proximal margin of the cranial articular process and forms 1/3 of the ventral trochlear margin. The olecranon is set off from caudal articular process of the phalanx by a rounded incision. The cranioproximal margin of the olecranon is almost semicircularly convex and caudally terminated in a tubercle. On the right wing finger this tubercle lies ventrally adjacent to the proximodistal corner of the basal phalanx of digit three. The cranial and caudal margins of the proximal articular head almost symmetrically converge in distal direction. In the middle, the shaft reaches its minimum diameter, which is half of the proximal one. From there, the shaft gradually diverges again to the distal articulation, whereby the cranial margin remains straight and slightly curves caudally directly at the articulation. The caudal margin of the shaft is slightly concave. This concavity increases at the distal articulation, which therefore is expanded caudally by 1/3 of its long axis. The ventral suture of the distal articulation is slightly convex and stands at a right angle to the long axis of the shaft. This orientation of the interphalangeal joints is also seen in the articulations further distally. The second wing finger phalanx is best seen on the left wing where only the middle part of the shaft is overlain by the humerus and the second phalanx of the right wing. The distal third of the right, second phalanx is obscured by the right radius/ulna and the thorax.

The ventral margin of the proximal articular head of the second phalanx is slightly concave. While the cranial margin of the shaft remains straight with the exception of a low proximal bulge, the caudal margin is concave. This concavity is wide and shallow at the proximal articulation and strongest at the distal joint, the cranial half of which is obscured by the proximal joint of the third phalanx on the left wing. The minimum diameter of the shaft is in its distal third, where it is about 1/3 of the diameter at the proximal articulation. The distal articulation is half the size of the proximal one. The shape of the third phalanx, which is only visible in the left wing, is identical with that of the second phalanx. On the right, only its distal half is seen. The third phalanx is 1/3 smaller and the caudal curvature of the shaft is slightly stronger. The proximal half of the fourth wing finger phalanx resembles that of the third, but the circumference of the proximal articular head is a little more exalted and set off from the shaft, which converges from there toward its blunt distal tip, which has 1/5 the width of the phalanx at the proximal articulation. The curvature of the shaft is a little stronger than that of the third phalanx.

Hind limb (Figs. 2, 3, 5)

Femur

The right femur is seen from laterally, the left from medially. The head and neck of both are obscured and the trochanteric area is partially damaged as is the knee joint. The fourth trochanter arises as a shallow convexity on the caudolateral face of the proximal fifth of the femur. It is confluent with a trochanteric crest that curves in proximodorsal direction around a ventrally facing protuberance, which could represent the 3rd trochanter. The dorsomedially protruding bulge is likely to be the base of the collum. Distal to the fourth trochanter, the shaft reduces its diameter by 1/3 and retains this thickness until the epicondyles. The cranial margin of the condyles is evenly convex. This convexity extends a little onto the dorsal face of the shaft. The condylar area is obscured in both femora by the tibial heads. The proximal half of the medial face of the right femur shows a low and blunt ridge.

Tibia

The left tibia is seen from craniomedially the right from craniolaterally. The distal 8th of the shaft of the left tibia is overlain by the right metatarsus. The tibia is more than 1/3 longer than the femur. The tibial head is three times as wide as the narrowest part of the shaft proximally adjacent to the distal roller. The articular surface of the tibial head is at a right angle to the long axis of the shaft. From the circumference of the articulation surface the tibia converges distally, whereby the lateral margin is stronger inclined than the medial one, which bears a medially orientated fibular tubercle with which the fibular head articulates. Toward distally, the fibular tubercle continues in a fibular crest, which mantles the proximal fifth of the shaft of the fibula. From the craniomedial two-thirds of the circumference the cnemial crest arises. Its distal half slightly curves medially. Lateral to this curvature, there is an elongate depression that extends half of the length of the cnemial crest. The crest runs along the medial margin of the tibial shaft, where it fades at the middle.

The shaft of the tibia gradually converges toward distally and shows a slight lateral curvature and diverges again to the distal roller, which is as wide as the proximal articulation. The cranial faces of the distal condyles are oval, with their long axes orientated parallel to the long axis of the shaft. They are separated by a deep intercondylar incision, which continues as a sulcus onto the distal extremity of the cranial face of the tibial shaft. Medially and laterally, this sulcus is bordered by sharp ridges that converge toward proximally, but together with the sulcus merge with the shaft before they meet. While the medial epicondylus lies in line with the medial margin of the tibial shaft, the medial margin of the lateral condyle lies in line with the lateral margin of the tibia.

Fibula

Only the left fibula is visible in cranial view and lies adjacent to the proximal fourth of the tibia. The lateral part of the head of the fibula and the proximolateral fifth of its shaft are obscured by the fibular tubercle and the fibular crest of the tibia. Level with the distal end of the fibular crest of the tibia, the medial margin is concave. Distal to this concavity, the shaft reaches its maximum visible thickness. From here toward distally, the shaft gradually converges into the fibular spine. The interosseal foramen opens immediately distal to the fibular crest of the tibia and is widest at the maximum diameter of the fibula. The interosseal foramen has half the length of the fibula. The visible part of the fibular spine terminates at the proximal fourth of the tibial shaft.

Tarsus

Only astragalus and calcaneum can be identified as separate bones and this only in the right pes with certainty. Both are preserved in plantar view. The calcaneum lies medial to the astragalus and has a rounded trapezoidal outline. The proximal margin is about twice as wide as the cranial margin and the medial and lateral margins are twice as long as the proximal one and slightly laterally convex. Along the longitudinal midline of the ventral face of the calcaneum runs a sinusoid groove. The astragalus lies laterally adjacent to the calcaneum. It is elongated rounded pentagonal in outline. Its medial margin is the longest and is concave such as the cranial margin, which is 1/3 the length of the medial one. The caudal margin has the same length, but is convex. A ridge runs transversely across the ventral face of the astragalus. In the right pes there are two cotyles separated by a longitudinally running ridge. It is likely that this structure is the proximal articulation surface of both calcaneum and astragalus, but the suture between the two is not seen. The three distal tarsals are seen as a transverse line of globular bones distally adjacent to the left calcaneum astragalus complex.

Metatarsus

The proximal articulation head of the metatarsals are obscured by their articulation with the distal tarsals and by their mode of overlapping, whereby the medial part of the heads of metatarsals II through V overlies the medial parts. Therefore, just the sharply rounded proximolateral corners of metatarsals I through IV are visible; metatarsal V is fully exposed. Most metatarsals are seen in plantar view. Only metatarsal I of the right pes is seen in plantolateral view. The shafts of metatarsals I, II and III are straight; that of metatarsal I is slightly sinusoid with a medially orientated curvature in its proximal half. From their proximal articulation metatarsals I through IV symmetrically converge in the proximal fifth to two-thirds of their articular diameter as reconstructed. The medial and lateral margins of the metatarsal shafts are parallel. They diverge just proximal to their distal roller joints, their epicondyles are 1/4 wider than the shafts. The metatarsus as a whole has just 1/6 the length of the tibia. Metatarsal II is the longest. Metatarsal I is only very slightly shorter. Metatarsal IV is 1/7 shorter than metatarsal II and metatarsal II is 10% shorter. The diameter of the shafts of these metatarsals is equal.

The fifth metatarsal is rounded triangular in outline and has 1/6 the length of metatarsal IV. Its proximal terminus is rounded and twice as wide as the shafts of the other metatarsals. A proximally pointing process arises from the proximal fourth of the lateral margin of metatarsal V, which overlaps the proximomedial corner of metatarsal IV

distally to the hook-shaped process, metatarsal V tapers toward its distal terminus.

In the right pes, metatarsals I and II as well as II and III include an angle of about 10°. Between metatarsal III and IV the angle is 5°. Metatarsal V lies adjacent to the lateral margin of metatarsal IV. Metatarsals I and II of the left pes lie adjacent to each other. Together, they form an angle of about 8° with metatarsal III. The angle between metatarsals III and IV is 10° and metatarsal V is angled medially at 5°.

Phalanges

All non-ungual pedal phalanges are exposed in plantar aspect. In the left pes, those of digits I through III are slightly dislocated from their metatarsals. With the exception of the phalanx of digit V, all pedal phalanges share the same overall shape but differ in their proportions. Between the articular ends, the lateral and medial margins of the shafts converge to a minimum transverse diameter in the middle. The ventral faces of the shafts show a longitudinally running shallow groove and are transversely slightly concave. The concavity is strongest in their proximal third. The proximal articulation of the non-ungual phalanges is concave in ventral view and about 1/3 wider that the smallest diameter of the shaft. The distal articulation is a double roller with a wide intercondylar sulcus. The ventral faces of the condyles are seen as tiny longitudinal protuberances on the craniomedial and craniolateral corners of the phalanges.

The left basal phalanges of digits I and II are of equal size and the longest. The basal phalanx of digit IV is 1/5 shorter than basal phalanx II. All of them are about 1/3 of the length of their metatarsals. In the left pes, basal phalanges I through III are of equal length. Basal phalanx IV is a little longer than the others, except the fifth, which is a tiny conical element of half the length of basal phalanx I.

In the second phalangeal row of both pedes that of digit III is the longest. The second phalanx of digit II is slightly shorter. In the right pes, the second phalanx of digit IV has just half the length of the second phalanx of digit II. This element is not seen in the left pes. Here, the second phalanx is as long as that of the third digit. Therefore, a third phalanx only exists in digit V of the left pes, which is a little longer than the second phalanx of the same digit.

The ungual phalanges are identical in size and shape. Those of digit I in the right and of digits III and IV in the left pes are seen from medially, that of digit I of the left pes in lateral view. The ungual phalanges of the right digits III and IV are exposed in plantar view. The right ungual phalanx of digit II is seen from plantomedially, that of digit IV in the right pes from plantolaterally. The unguals show a slightly convex dorsal and a slightly concave ventral margin. The dorsal two-thirds of the proximal margin are concave. The proximal plantar margin of the trochlea is concave as well. This part represents the lateral or medial margin of the ungual trochlea. Plantar to the trochlea there is a small adductor tubercle, which makes 1/3 of the proximal margin and protrudes in proximoplantar direction. Distally the adductor tubercle merges with the slightly concave sole of the unguals. A sulcus separates the adductor tubercle from the dorsal part of the unguals both medially and laterally. The medial and lateral margins converge toward the apex and are slightly convex.

Pes as an entity

Taking all phalanges together, the fourth digit is the longest. Toward laterally, they become gradually shorter, whereby the difference between digits I and II is 1/3, by far the shortest digit is the fifth. When adding the metatarsals, the pedal rays II and II are of equal length, the fourth is a little shorter and the first again is a little shorter than the fourth. The fifth pedal ray is by far the shortest of all with less than 1/5 the length of the first pedal ray.

Individual age and sex

The partial fusion of the glenoideal suture of the scapulocoracoid and the near complete co-ossification of the olecranon process with the basal wing finger phalanx suggests a late juvenile or subadult individual (cf. Bennett 1993; Frey and Martill 1998). The puboischiadic symphysis of NMB Sh 110 is fused like in the tapejarid SMNK-PAL 4331 and *Barbosania gracilirostris* Elgin and Frey 2011 (MHNS 1082 00/85), while in other pterosaur specimens this symphysis is open, e.g., in the ornithocheirid SMNK-PAL 1133 (all from the Late Cretaceous Santana Formation, NE Brazil). We suggest here that a ventrally open pelvis lacking a puboischiadic symphysis would be indicative for a female because of the wide pelvic apperture would serve as an egg passage (Unwin 2006). Those pterosauria with a tightly fused puboischiadic symphysis and a narrow pelvic aperture like NMB Sh 110 are likely to have been males.

Comparisons

Apart from differences in biometry and wing articulation, *Aurorazhdarcho* shows significant anatomical differences to all other Pterodactyloidea of the Late Jurassic. Most, if not all of these anatomical differences have implications on the flight mechanics of the animal and are therefore discussed in the context of constructional morphology. About 35 pterosaur taxa, which are referred to the Pterodactyloidea are known from the Late Jurassic (Tithonian) or the

Early Cretaceous (Barremian). Of these, the following are complete enough for a comparison with *Aurorazhdarcho*.

Ctenochasmatidae: *Beipiaopterus chenianus* Lü 2003, *Ctenochasma elegans* Wagner 1861, *Ctenochasma gracile* Oppel 1862, *Gnathosaurus subulatus* Seeley 1869, *Gnathosaurus macrurus* Seeley 1869, *Huanhepterus quingyangensis* Dong 1982;

Gallodactylidae (= Ctenochasmatoidea *incertae sedis* (Unwin 2003): *Cycnorhamphus canjuersensis* Fabre 1974, *Cycnorhamphus suevicus* Quenstedt 1855;

Germanodactylidae: *Germanodactylus cristatus* Wiman 1925, *Germanodactylus rhamphastinus* Wagner 1851;

Pterodactylidae: *Pterodactylus longicollum* von Meyer 1854, *Eosipterus yangi* Ji & Ji 1997, *Pterodactylus antiquus* Cuvier 1809, *Pterodactylus grandipelvis* von Meyer 1859–1860, *Pterodactylus kochi* Wagner 1837, *Pterodactylus micronyx* von Meyer 1862.

In the Late Jurassic among pterodactyloid pterosaurs a variety of morphotypes exist with respect to the biometry of the apendicular skeleton. In *Pterodactylus*, *Germanodactylus*, *Cycnorhamphus, Ctenochasma elegans, Eosipterus, Huanhepterus* and *Beipiaopterus*, the main lift generating area exceeds the main lift area in relative length. It is equal in length to the main lift area in *Auroazhdarcho* and a little shorter in *Ctenochasma elegans*. The reduction of the main propulsion area with respect to the main lift area is significantly combined with the elongation of the wing finger metacarpus, femur and tibia, resulting in a decrease of the aspect ratio, an increase of the size of the uropatagium and increased mobility of the trailing edge at least in the main lift area. In the Cretaceous this tendency continues only in the azhdarchoid pterosaur constructions like *Zeijangopterus*, *Chaoyangopterus, Tupuxuara* and *Tapejara*. A low wing attachment and likely an increased manoeuvrability are mandatory in the azhdarchoid type of construction (Frey et al. 2003a). All other known groups of Cretaceous pterosaurs, e.g., ornithocheirids, pteranodontids and nyctosaurids show a high aspect ratio, which is either brought about by an elongation of the wing finger metacarpal (nyctosaurids) or the wing finger (ornithocheirids) or both (pteranodontids).

Ctenochasma elegans and *Aurorazhdarcho* are very close to each other concerning their limb bone biometry, the morphology of the three medial digits of the manus and the dimensions of the skull as concluded from the touch down mark in *Aurorazhdarcho*. However, no specimen of *Ctenochasma elegans* preserves the shoulder girdle in a way that the wing articulation can be reconstructed with reliability. The low wing attachment as is seen in *Aurorazhdarcho*, however, is an essential feature of the azhdarchoid type of pterosaurs. Furthermore, the genus *Ctenochasma* in most cladograms and other systematic analyses is grouped next to *Pterodactylus*. This can not be confirmed on constructional evidence upon which we base the new genus and species *Aurorazhdarcho primordius*.

Only one questionable azhdarchoid remain is known from the Late Jurassic of Europe until now. It comprises an elongate cervical vertebra, a wing finger phalanx and some bone fragments from the Purbeck Limestone and is referred to *Doratorhynchus validus* Seeley 1875.

Ratios between the wing elements

Aurorazhdarcho is the only known Late Jurassic pterodactyloid, in which the length of the metacarpal is equal to the length of radius and ulna. Also unique is that the first wing finger phalanx is the longest element in the wing (Table 1; Fig. 6). The distally positioned wing finger articulation results in an extension of the proximal part of the wing, where a direct muscular control occurs (Bennett 2003; Frey et al. 2006). At the same time, the relative distance between the interphalangeal joints of the wing finger is reduced, which decreases the lever forces acting on the most basal interphalangeal wing finger joint. Such a lever arm system would be the precondition for an actively controlled wing with a short wing finger relative to the brachium and metacarpus with reduced distal wing finger components as is seen in Cretaceous azhdarchids (Frey et al. 2003a). During terrestrial locomotion, the stride of the arms is longer than in any other Jurassic pterodactyloid and possibly wider than the stride in non-azhdarchomorph constructions. Another unique feature is the short and stubby small digits of the manus with respect to the length of the metacarpus.

Ratios between the hind limb elements

The ratio between femur and tibia is similar to that of other Jurassic pterodactyloids, however the pes is 1/3 shorter when compared to the Jurassic pterodactyloid average. If the pes is invoked in steering, the effective surface would be smaller than in any other Jurassic pterodactyloid (Table 1; Fig. 6).

Ratios wing/hind limb

The hind limb of *Aurorazhdarcho* is longer relative to the wing compared to any other pterodactyloid of the Late Jurassic, including *Pterodactylus*. This would correlate with a generally longer stride during terrestrial locomotion combined with small autopodial imprints with the belly high above ground. Due to the long hind limbs, the proximal part of the wing is deep with respect to the lateral extension, resulting in a low aspect ratio (Fig. 6).

Low wing articulation, deltopectoral crest and sternocoracoideal articulation

The most remarkable feature of *Aurorazhdarcho* is the low wing attachment combined with a subrectangular deltopectoral crest arising from the proximal fourth of the humerus. The effect of a low wing attachment is an increase of manoeuvrability with the option to stable gliding (Frey et al. 2003a). This construction has been only recognised in azhdarchoid pterosaurs until now, where it is aligned with a low lever attachment of the pectoral musculature by means of a subrectangular deltopectoral crest on the humerus (Lawson 1975; Langston 1981; Nessov 1984; Frey et al. 2003a), which allows a more powerful down-stroke. The wide furca of the coracoid, which is present in *Aurorazhdarcho*, *Tapejara* and *Quetzalcoatlus*, allows rotation movements of the entire shoulder girdle to a limited degree, which helps to increase the options for wing adjustment at its articulation (Frey et al. 2003a). Thus, the *Aurorazhdarcho* construction would be a potential preconstruction of the Cretaceous azhdarchoid pterosaurs.

Problems with cladistic analysis

In all published cladistic analyses, the Azhdarchoidea form a well-defined and distinct group within the Pterosauria (e.g. Kellner 2003; Unwin 2003; Lü and Ji 2006). However, in the case of *Aurorazhdarcho* only the postcranial characters are relevant. All together 27 postcranial character sets were defined, comprising characters of the skeleton in general (2), scapulocoracoid (3), sternum (1), humerus (2), deltopectoral crest (1), ratios within front limb (5), pteroid (2), metacarpus (2), ratio front limb/hind limb (5), ratios within hind limb (1) and hind limb (4). Of these only 6 are unique to *Aurorazhdarcho*, 3 are shared with "basal azhdarchids", 3 are intermediate and 5 are vicariating throughout the group. Thus, there is strong evidence that *Aurorazhdarcho* would become the sister clade of the Azhdarchoidea, or, possibly, a basal member of the group. The question might arise, why we do not prove evidence by applying a cladistic analysis to the postcranium of *Auroazhdarcho*. The main reason is that the low wing attachment is reason enough to align the specimen with the azhdachoid construction, which separates the group from all other Pterosauria. Hence, we additionally see some methodological problems in the characters defined for Pterosauria in general. Fourteen of all postcranial characters refer to osteological ratios. Here, we discuss these characters in the context of possible functional coupling, which makes most of them obsolete for a cladistic analysis.

1. The ratio between the length of scapula and coracoid determines the position of the wing articulation level. It is therefore directly aligned with the flight mechanics. If the low position of the glenoid fossa is regarded as original tetrapod, the azhdarchoid pterosaur construction has retained the low articulation of the front limbs and thus must have separated in the early history of the Pterosauria, possibly during the Triassic. Then, the high wing articulation could have evolved several times independently within the Pterosauria. If the low wing articulation is regarded as derived, the re-development of the primitive position of the glenoid fossa has to be explained. To resolve this question, a reinvestigation of the shoulder girdle of early Pterosauria would be necessary. For now, this problem remains unresolved pending an engineering approach concerning the consequences of low wing attachment, too. Hence, the character should be dismissed because of its evident functional impetus and unclear origin (Frey et al. 2003a). However, the low wing attachment might result in mechanical consequences that determine the configuration of at least two further characters: the shape of the deltopectoral crest and the sternum. The ventral curvature of the deltopectoral crest in the humerus in Azhdarchoidea is directly aligned with the arrangement of the pectoral muscle masses. Due to the fact that the low wing attachment has an influence on the topography of exactly this muscle mass, a functional relationship between the low wing attachment and the form of the deltopectoral crest appears more than likely, especially if a muscular modification in advanced Azhdarchoidea is evidenced by crests and flanges on the scapulocoracoid near the glenoid fossa, which never occur in other pterosaur constructions. As for *Aurorazhdarcho*, there is neither a deflection of the deltopectoral crest nor an ornamentation on the scapulocoracoid like in many other Pterosauria, reflecting a primordial azhdarchoid condition, as does the missing pneumatic foramen in the neck of the humerus. The low wing attachment indicates a change in muscle arrangement towards a low lever system, which may only work with a deltopectoral lever on the humerus. Mechanical investigations concerning this system are under study, but due to the coupling of shoulder construction, pectoral muscles and humeral levers, the shape of the deltopectoral crest should be dismissed as a character for a cladistic analysis. The same holds true for the sternal crest. In all azhdarchoid constructions with preserved sterna this crest is short but deep compared with that of other pterosaurs. This is mostly aligned with a short and shovel-shaped sternal plate. Apparently the deep sternal crest allows an elongation of the cranial pectoral muscle fibres in the context of low wing attachment. The possible migration of some adductor muscles onto the coracoid may result in the option to

decrease the surface of the sternal plate. The consequence of the general length reduction of the azhdarchoid sternum is a concentration of the flight muscles around the centre of gravity and a more direct action vector.

2. Changes in the ratios within the bones of the brachium are influencing the entire lever system of the wing. However, only in a few cases, consequences on the flight mechanics can be reconstructed. While the length of the humerus and radius/ulna with respect to each other and the body length varies only little, there is a tendency to increase the length of the metacarpals and the basal wing finger phalanx in several groups within the Pterosauria (pteranodontids, nyctosaurids and azhdarchoids, but also taxa like *Cycnorhamphus* and *Ctenochasma*). The elongation of the metacarpal shifts the wing finger articulation distally. This increases the main lift area of the wing. Often, especially in azhdarchoids and nyctosaurids the distal wing finger phalanges are reduced in length with respect to the basal one, resulting in a decrease of the main thrust generation area, but only in azhdarchoids this is combined with an elongation of the hind limbs, especially the tibia. Thus, it appears evident that many proportional shifts of wing elements result in areodynamical changes and thus should be regarded as an entity. Hence, not only detailed studies on the flight mechanics with respect to the mobile elements in the wing are pending, but also the range of mobility in single joints in most taxa is unknown (Wilkinson et al. 2006; Bennett 2007), as is the position of the wing elements during flight.
3. The pteroid and its biomechanical role has been and still is under debate (Bennett 2001a, Bennett 2001b, 2006, 2007 and Frey et al. 2006 *contra* Frey and Riess 1981 and Wilkinson et al. 2006). The carpal osteology of *Aurorazhdarcho* shows that the notch of the preaxial carpal houses a sesamoid bone (see above) and that the pteroid articulates in a socket formed by the proximal and distal syncarpal (Fig. 7). The tip of the pteroid thus faces proximally towards the shoulder. The length of the pteroid therefore indicates, how many percent of the propatagium form a stiff leading edge. If the pteroid is mobile, it could control tension and probably camber of the forewing. The consequences on the flight of pterosaurs are hitherto unclear, and subject to investigation. However, the pteroid bone as part of the wing cannot be regarded as a separate character set and thus should not be used for a cladistic analysis.
4. Ratios between hind limb bones either concern the relative length of the pes with respect to the tibia or that of the tibia with respect to the femur. Due to the fact that the brachiopatagium attaches to the ankle most likely in all Pterosauria (Tischlinger and Frey 2002; Frey et al. 2003b), the relative length of the femur determines the depth of the proximal part of the wing and the uropatagium. If pterosaurs held their hind limbs in a lateral position similar to bats, the tibia could have acted as a lever, which rotated around the femoral long axis in the acetabulum. If so, tibial rotation can be used for the control of the membrane tension, or had an elevator or aileron function (Frey et al. 2003b). Provided the pes is held vertically during flight, its size might be a scale for the efficiency as a rudder or air brake respectively. The hind limb thus acts as an entity within the flight apparatus and consequently the character sets should not be separated. However, the hind limb position during flight until now is speculative and needs to be resolved with the help of aerodynamics and engineering methods.
5. The ratio between the length of front and hind limb is a direct indicator for the aspect ratio of the pterosaurian wing. Among the Azhdarchoidea there is a shift towards a low aspect ratio construction, where a large hind limb is combined with a short wing finger with respect to the proximal arm elements. In *Aurorazhdarcho* this tendency is visible when compared to other Late Jurassic pterosaurs (Fig. 6) In advanced azhdarchoids, there is a combination of a short thrust generating wing segment distally with a deep and long lift generating proximal part of the wing with a large surface uropatagium. The depth of the lift generating area is determined by the concavity of the trailing edge of the brachiopatagium, which is unknown in azhdarchids at present. Probably this wing construction was suitable for high performance gliding combined with manoevrability, as was previously suggested (Frey et al. 2003a). Hence, this hypothesis has to be verified. Under the aspect of a mechanical correlation of wing and hind limb the use of the character sets referring to the ratio between front and hind limbs are questionable.

With respect to possible functional dependencies of most postcranial bones of the 27 character sets only three remain plausible: the wall thickness of the bones, the ventral pneumatic opening on the humerus and the reduction of the metacarpals I-III from proximally. These character sets cannot be directly linked with flight mechanics. Of these three, the pneumatic opening and the reduction of the matacarpals I–III would be relevant for diagnosing the Azhdarchoidea. The presence or absence of a ventral pneumatic opening is vicariating within the group (Kellner 2003; Unwin 2003; Lü and Ji 2006). Concerning the reduction of the metacarpals I–III, *Aurorazdarcho* shows only a reduction of the first, which could be

interpreted as a primordial stage for further reduction, possibly in the context with the elongation of the wing finger metacarpal. However, such a reduction is not seen in pteranodontids and nyctosaurids with elongate wing finger metacarpals, too. Therefore, there is no evidence of a functional aspect aligned with the reduction of the metacarpals I–III at present.

According to classical comparative anatomy combined with a biomechanical approach *Aurorazhdarcho* represents an early azhdarchoid construction, which sets the basal level for the evolution of the Azhdarchoidea. Phylogenetic relationships cannot be established with the given data sets. For any analysis it is not sufficient to refer to the osteology only. The mechanical context of character sets can only be evaluated, when soft tissue is included in an analysis.

Taphonomy

According to the state of articulation combined with the touch down mark of head and neck, the carcass arrived at the bottom of the lagoon in an early stage of decay, possibly after a few days of floating (Kemp 2001). It appears likely that the carcass came down with the right shoulder and the proximal elements of right wing first. The disarticulated distally pointing pteroid bone suggests a rupture of the propatagial tendon. The left wing finger must have pointed into the water column in a cross-over position with the right wing finger. The hind limbs most likely were primarily both afloat, as were the left wing, head and neck. The trunk rested on its ventral left side. Evidently, there must have been a primary torsion at the cervicothoracical junction.

On the seafloor, decay must have continued, combined with gas formation in the thoracoabdominal cavity and a softening of the articular ligaments (e.g. Weigelt 1927; Polson and Gee 1973). After the thigh musculature became liquidised, the right hind limb sank down with a rotation in the hip joint of about 180° caudally, which caused the caudal orientation of the knee joint. The left hind limb followed shortly after with the same type of caudal rotation. The most viable joint in the hind limbs are the knee joints and the joints of the pes. The most flexible one would be the tibiotarsal articulation. The head of both femora must have been held in place by a ligamentum teres, which allowed torsion but no disarticulation.

The left wing moved medially in the glenoid fossa, whereby the left humerus sank across the thorax at a right angle. The lower arm and the carpus turned caudally. The slight disarticulation of the left elbow joint indicates a more advanced state of decay than in the right wing, apparently a result of floating. When the wing finger of the left wing finally sank, it took the right wing finger down, which probably was tangled in remnants of the wing membranes. This could explain the hyperextension of the digital phalanges of the both wing fingers.

The terminal left wing finger phalanx lies under the ventral margin of the cranial touch down mark. Therefore, the last parts to touch down were head and neck. However, head and neck remained mostly floating, but probably touched down several times before the connection between thorax and neck failed. Flakes of skin came off and got stuck in the sediment, where the touchdown took place. Finally, neck and head drifted away. The most likely scenario for the lift-off of the head is the formation of gas. This could happen in the cranial and cervical air sacs, the narial cavity, the braincase, and the eyeballs.

Decay gases also caused the explosion of the abdomen. The abdominal wall ruptured between the caudal margin of the sternum and the cranial margins of the prepubic bones and left the gastralia scattered around the rupture. During this phase the sternocostal articulations failed too, and the body as a whole slid to the right side over the sternum, accompanied by a gentle degassing through the cranial thoracic aperture. However, the abdominal musculature must have been still viable in the area of the prepubic bones, which remained in place during the collapse of the thorax, before they were pressed into the abdominal cavity, likely due to compaction.

As previously suggested, the cervicothoracic articulation was most likely primarily damaged. The reasons for this assumption are the torsion between the body and the neck, the ruptured right propatagial tendon. Finally, the loss of neck and head would be difficult to explain, if the articulations of vertebral column of the neck would have been still as viable as was the rest of the skeleton. Further hints to a primary damage at the base of the neck are the disarticulated right scapulocoracoid and the rotational displacement of the first thoracic vertebra to the right side. Due to the general state of preservation, the disarticulation of neck and head from the carcass cannot be a result of scavenging or decay. More likely, the pterosaur was subject to a mechanical distorsion of the head and the neck, resulting in a violent disarticulation of the neck from the thorax with skin and ligament rupture. The fact that under these circumstances the degassing happened through the abdomen can only be explained by a diaphragma separating the thoracic from the abdominal cavity.

Actuotaphonomic experiments have shown that larger animals tend to sink slower than smaller ones (Kemp 2001). However, we can assume that the pneumatic skeleton of pterosaurs would float longer than that of other tetrapods (lizards, turtles). Given the state of articluation of the present specimen, a fast sinking must be propagated, most likely due to post mortem primary gas loss in thorax and neck as a result of injury as is observed in birds (Davis

and Briggs 1998). In this context it is interesting to note that from all tetrapods in the Solnhofen area, completely articluated pterosaurs make up more than 60% (Kemp 1999), although large specimens tend to be rare. Furthermore, fossil lagerstätten where well preserved pterosaurs are common tend to have a high diversity of preserved flying insects (e.g., Crato Formation, see Martill et al. 2008). Kemp (2001) explained this well know fact by catastrophic input due to storms and waves. However, the massive damage makes it more likely, that the animal was attacked by a predator that grabbed the neck and tried to take the pterosaur apart. The prey was lost and immediately sank to the ground.

Conclusions

Aurorazhdarcho primordius n.gen. n.sp. from the Late Jurassic of the Eichstätt (Bavaria, Southern Germany) area indicates an Eurasian origin of Azhdarchoidea. All other known species of this group come from Early Cretaceous deposits of either Gondwana (e.g., Brazil, Jordan, Morocco) or the Eurasian Late Cretaceous (e.g. USA, Hungary, China). The evidence that *Aurorazhdarcho* represents the most basal azhdarchoid known comes not only from its specific azhdarchoid character set combined with transitional and basal characters, but also from the mechanical context concerning the characteristics of the azhdarchoid flight apparatus, which appears unique among the Pterosauria. The analysis also shows that most postcranial characters used in cladistic analyses should be withdrawn due to mechanical coupling.

The presence of skin flakes that outline the head of the pterosaur and the almost articulated preservation of the specimen are best explained by an unsuccessful attack of a predator resulting in a fast sinking of the carcass. This kind of preservation has never been reported from the Solnhofen limestone before.

Acknowledgments We express our sincere gratitude to the Freiwillige Museumsverein Basel, for acquiring the specimen on the behalf of the Natural History Museum Basel, where it is deposited. We thank Christopher Bennett (Fort Hays State University, Hays) for his excellent, helpful and constructive comments. We furthermore thank an anonymous reviewer for valuable comments on the manuscript especially with respect to the possible relationship of NMB Sh 110 and *Pterodactylus longicollum* and *P. micronyx*. Jean-Paul Billon-Bruyat (Paléontologie A 16, Porrentruy) did an excellent job as an editor. Many thanks for this.

References

Bennett, S. C. (1993). The ontogeny of *Pteranodon* and other pterosaurs. *Paleobiology, 19*, 92–106.

Bennett, S. C. (2001a). The osteology and functional morphology of the Late Cretaceous pterosaur *Pteranodon.* Part I. General description of osteology. *Palaeontographica, A260*, 1–112.

Bennett, S. C. (2001b). The osteology and functional morphology of the Late Cretaceous pterosaur *Pteranodon.* Part II. Size and functional morphology. *Palaeontographica, A260*, 113–153.

Bennett, S. C. (2003). Morphological evolution of the pectoral girdle of pterosaurs: Myology and function. In E. Buffetaut & J.-M. Mazin (Eds.), *Evolution and palaeobiology of pterosaurs* (pp. 191–215). London: Geological Society of London, Special Publications 217.

Bennett, S. C. (2006). Articulation and function of the pteroid bone of pterosaurs. *Journal of Vertebrate Paleontology, 26*(suppl. 3), 41A.

Bennett, S. C. (2007). Articulation and function of the pteroid bone in pterosaurs. *Journal of Vertebrate Paleontology, 27*, 881–891.

Davis, P. G., & Briggs, D. E. G. (1998). The impact of decay and disarticulation on the preservation of fossil birds. *Palaios, 13*, 3–13.

Elgin, R. A., & Frey, E. (2011). A new ornithocheirid, *Barbosania gracilirostris* gen. et sp. nov. (Pterosauria, Pterodactyloidea) from the Santana Formation (Cretaceous) of NE Brazil. *Swiss Journal of Palaeontology*. doi:10.1007/s13358-011-0017-4

Frey, E., Buchy, M. C., & Martill, D. M. (2003a). Middle- and bottom-deckers Cretaceous pterosaurs: Unique designs in active flying vertebrates. In E. Buffetaut & J.-M. Mazin (Eds.), *Evolution and palaeobiology of pterosaurs* (pp. 267–274). London: Geological Society of London, Special Publications 217.

Frey, E., Buchy, M.-C., Stinnesbeck, W., González González, A., & Di Stefano, A. (2006). *Muzquizopteryx coahuilensis* n.g, n.sp., first evidence for the presence of nyctosaurid pterosaurs in the Coniacian (Late Cretaceous) of northeastern Mexico (Coahuila). *Oryctos, 6*, 19–39.

Frey, E., & Martill, D. M. (1998). Late ontogenetic fusion of the processus tendinis extensoris in Cretaceous pterosaurs from Brazil. *Neues Jahrbuch für Geologie und Paläontologie, Monatshefte 1998,* 587–549.

Frey, E., & Riess, J. (1981). A new reconstruction of the pterosaur wing. *Neues Jahrbuch Geologie Paläontologie Abhandlungen, 161*, 1–27.

Frey, E., Tischlinger, H., Martill, D. M., & Buchy, M.-C. (2003b). Specimens of Pterosauria (Reptilia) with soft parts with implications for pterosaurian anatomy and locomotion. In E. Buffetaut & J.-M. Mazin (Eds.), *Evolution and palaeobiology of pterosaurs* (pp. 233–266). London: Geological Society of London, Special Publications 217.

He, H. Y., Wang, X. L., Zhou, Z. H., Wang, F., Boven, A., Shi, G. H., et al. (2004). Timing of the Jiufotang Formation (Jehol Group) in Liaoning, northeastern China, and its implications. *Geophysical Research Letters, 31*, 1709.

Kellner, A. W. A. (1989). A new edentate pterosaur of the Lower Cretaceous from the Araripe Basin, Northeast Brazil. *Anais de Academia Brasileira de Ciencias, 61*, 439–446.

Kellner, A. W. A. (2003). Pterosaur phylogeny and comments on the evolutionary history of the group. In E. Buffetaut & J.-M. Mazin (Eds.), *Evolution and palaeobiology of pterosaurs* (pp. 105–137). London: Geological Society of London, Special Publications 217.

Kellner, A. W. A., & Campos, D. A. (2007). Short note on the ingroup relationships of the Tapejaridae (Pterosauria, Pterodactyloidea. *Boletim do Museu Nacional, 75*, 1–14.

Kemp, R. (1999). *Solnhofen tetrapod taphonomy*. Unpublished Ph.D. Thesis, University of Bristol.

Kemp, R. (2001). Generation of the Solnhofen tetrapod accumulation. *Archaeopteryx, 19*, 11–28.

Langston, W. (1981). Pterosaurs. *Scientific American, 244*, 93–102.

Lawson, D. A. (1975). Pterosaur from the latest Cretaceous of West Texas. Discovery of the largest flying creature. *Science, 187*, 947–948.

Li, J., Lü, J., & Zhang, B. (2003). A new lower Cretaceous sinopterid pterosaur from the Western Liaoning, China. *Acta Palaeontologica Sinica, 42*, 442–447.

Lü, J., Gao, Y., Xing, L., Li, Z., & Sun, Z. (2007). New species of *Huaxiapterus* from the Early Cretaceous of western Liaoning. *Acta Geologica Sinica (English edition), 81*, 683–687.

Lü, J., & Ji, Q. (2005). A new Azhdarchid pterosaur from the Early Cretaceous of Western Liaoning. *Acta Geologica Sinica, 79*, 301–307.

Lü, J., & Ji, Q. (2006). Preliminary results of a phylogenetic analysis of pterosaurs from western Liaoling and surrounding areas. *Journal of the Paleontological Society of Korea, 22*, 239–261.

Lü, J., Jin, X., Unwin, D. M., Zhao, L., Azuma, Y., & Ji, Q. (2006). A new species of *Huaxiapterus* (Pterosauria: Pterodactyloidea) from the Lower Cretaceous of western Liaoning, China with comments on the systematics of tapejarid pterosaurs. *Acta Geologica Sinica, 80*, 315–326.

Lü, J., Unwin, D. M., Xu, L., & Zhang, X. (2008). A new azhdarchoid pterosaur from the Lower Cretaceous of China and its implications for pterosaur phylogeny and evolution. *Naturwissenschaften, 95*, 891–897.

Lü, J., & Yuan, C. (2005). New tapejarid pterosaur from Western Liaoning, China. *Acta Geologica Sinica, 79*, 453–458.

Martill, D. M., Bechly, G., & Loveridge, B. (2008). *The Crato Fossil Beds of Brazil. Window into an ancient world* (p. 624). Cambridge: Cambridge University Press.

Martill, D. M., Frey, E., Sadaqah, R. M., & Khoury, H. N. (1998). Discovery of the holotype of the giant pterosaur *Titanopteryx philadelphiae* ARAMBOURG 1959, and the status of *Arambourgiania* and *Quetzalcoatlus*. *Neues Jahrbuch Geologie Paläontologie Abhandlungen, 207*, 57–76.

Nessov, L. A. (1984). Pterozavryi i ptitsyi pozdnyevo myela sryednyei Azii (Upper Cretaceous Pterosaurs and birds from central Asia). *Paleontologisheskiy Zhurnal, 1*, 47–57.

Nessov, L. A. (1991). Giant flying reptiles of the family Azhdarchidae: I. morphology and systematics, Vestnik. *Leningradskogo Universiteta. Seriya. 7; Geologiya, Geografiya 2*, 14–23 (in Russian).

Polson, C. J., & Gee, D. J. (1973). *Drowning in the Essentials of Forensic Medicine* (3rd ed., pp. 440–466). Oxford: Pergamon Press.

Schweigert, G. (2007). Ammonite biostratigraphy as a tool for dating Upper Jurassic lithographic limestones from South Germany—first results and open questions. *Neues Jahrbuch für Geologie und Paläontologie, Abhandlungen, 245*, 117–125.

Tischlinger, H. (2002). Der Eichstätter *Archaeopteryx* im langwelligen UV-Licht. [The Eichstätt specimen of *Archaeopteryx* under longwave ultraviolet light]. *Archaeopteryx, 20*, 21–38.

Tischlinger, H. (2005). Ultraviolet light investigations of fossils from the Upper Jurassic Plattenkalks of Southern Frankonia. *Zitteliana B, 26*, 26.

Tischlinger, H., & Frey, E. (2002). Ein *Rhamphorhynchus* (Pterosauria, Reptilia) mit ungewöhnlicher Flughauterhaltung aus dem Solnhofener Plattenkalk. *Archaeopteryx, 20*, 1–20.

Unwin, D. M. (1995). Preliminary results of a phylogenetic analysis of the Pterosauria (Diapsida: Archosauria). In A. Sun & Y. Wang (Eds.), *Sixth Symposium on Mesozoic Terrestrial Ecosystems and Biota* (pp. 69–72). Beijing: Ocean Press.

Unwin, D. M. (2003). On the phylogeny and evolutionary history of pterosaurs. In E. Buffetaut & J. M. Mazin (Eds.), *Evolution and palaeobiology of pterosaurs* (pp. 139–190). London: Geological Society of London, Special Publications 217.

Unwin, D. M. (2006). *The pterosaurs: From deep time* (p. 347). New York: Pi Press.

Unwin, D. M., & Martill, D. M. (2007). Pterosaurs of the Crato Formation. In D. M. Martill, G. Bechly, & R. F. Loveridge (Eds.), *The Crato fossil beds of Brazil: Window into an ancient world* (pp. 475–524). Cambridge: Cambridge University Press.

Wang, X., & Zhou, Z. (2003a). A new pterosaur (Pterodactyloidea, Tapejaridae) from the Early Cretaceous Jiufotang Formation of western Liaoning, China and its implications for biostratigraphy. *Chinese Science Bulletin, 48*, 16–23.

Wang, X.-L., & Zhou, Z.-H. (2003b). Two new pterodactyloid pterosaurs from the Early Cretaceous Jiufotang Formation of Western Liaoning, China. *Vertebrata PalAsiatica, 41*, 34–41.

Wang, X., & Zhou, Z. (2006). Pterosaur assemblages of the Jehol Biota and their implication for the Early Cretaceous pterosaur radiation. *Geological Journal, 41*, 405–418.

Weigelt, J. (1927). Rezente Wirbeltierleichen und ihre paläobiologische Bedeutung. Leipzig: M. Weng.

Wilkinson, M. T., Unwin, D. M. & Ellington, C. P. (2006). High lift function of the pteroid bone and forewing of pterosaurs. *Proceedings of the Royal Society London B 273*, pp. 119–126.